



Effect of Molar Ratio and Calcination Temperature on Particle Size of CeO₂/γ-Al₂O₃ Nanocomposites Prepared via Reverse Micelle Process

R. Lotfi¹, S. Abedini Khorrami^{1*}, M. E. Olya², Sh. Moradi¹ and F. Motiee¹

¹ Department of Chemistry, North Tehran Branch, Islamic Azad University, P. O. Box: 19862-23698, Tehran, Iran.

² Department of Environmental Research, Institute for color science and technology, P. O. Box: 19584-26341, Tehran, Iran.

ARTICLE INFO

Article history:

Received: 11 Feb 2016

Final Revised: 29 Apr 2016

Accepted: 01 May 2016

Available online: 01 May 2016

Keywords:

Nanocomposite

Reverse micelle

Calcination temperature

Molar ratio

Cerium oxide

Aluminum oxide

ABSTRACT

A porous composite of cerium oxide and gamma aluminum oxide pigments was prepared via sol-gel processing controlled within reverse micelles of nonionic surfactant Triton X-114 in cyclohexane. The precursor was heated at several calcination temperatures between 823-1123K. This process includes three steps. In the first step of preparation the ceria sol was prepared. In the second step, cyclohexane was mixed with surfactant, distilled water and ceria sol. At last, gamma nano aluminum oxide was fluently injected into the mixture. The micellar ceria/γ-alumina sol precursor with different molar ratios was mechanically stirred to form a homogeneous suspension. The mixture was washed with ethanol. The effect of different molar ratios of Ce:Al on the crystallization was also studied. X-ray diffraction (XRD) analysis, transmission electron microscopy (TEM), scanning electron microscopy (SEM), temperature programmed reduction (TPR) technique and N₂ adsorption/desorption isotherm revealed that crystalline nanosized pigments are obtained. The produced pigments possess mesoporosity with pore diameters mainly distributed between 20 to 45 nm. Surface area increases by increasing the calcination temperature. Also, the particle size of the pigments decreases with increasing the Ce:Al molar ratio. Prog. Color Colorants Coat. 9 (2016), 109-116 © Institute for Color Science and Technology.

1. Introduction

Metal oxides play a very important role in many areas of chemistry, physics and materials science [1]. In technological application, oxides are used in sensors, fuel cells, pigments, coating for the passivation of surfaces against corrosion, fabrication of

microelectronic circuits and as catalysts [2, 3]. In order to display mechanical or structural stability, a nanoparticle must have a low surface free energy. As a consequence of this requirement, phases that have a low stability in bulk materials can become very stable

*Corresponding author: s_akhorrani@iau-tnb.ac.ir

in nanostructures. This structural phenomenon has been detected in Al_2O_3 [4, 5]. Size-induced structural distortions associated with changes in cell parameters have been observed, for example, in Al_2O_3 [4] and CeO_2 [6] nanoparticles.

Attention in the Al-O system is centered in the Al_2O_3 stoichiometry due to its importance as a catalyst component or absorbent and ceramic material in a multitude of industrial processes. Novel nanostructured alumina is currently used as a support for active phases in the field of catalysis or is coated with other materials [7]. Gamma alumina nanoparticles have been synthesized by various techniques such as: sol gel [8, 9], control precipitation [10], hydrothermal synthesis [11], flame spray pyrolysis [12], combustion synthesis [13, 14] and reverse microemulsion methods [15-19].

Ceria is an oxide with important applications in area of catalysis, materials science, pigments and photochemistry. In its most stable phase, bulk CeO_2 adopts a fluorite-type Fm3m crystal structure in which each metal cation is surrounded by eight oxygen atoms. Experimental and theoretical studies indicate that bulk CeO_2 is not a fully ionic oxide [20]. Nanoparticles of ceria have been studied in the area of pigments and catalysts [21]. In recent years, substantial progress has been made thanks to the use of better synthesis methods and advanced techniques for structural characterization [22]. It is not easy to find a synthesis method that provides ceria nanoparticles with small particle size (< 3 nm) and narrow size distribution [2, 23].

A number of research have been studied on parameters of reverse micelle synthesis of nanoparticles, usually controlled and manipulated during design procedures, including molar ratio of surfactant to co-surfactant [24], water to surfactant [25, 26], surfactant effect [27], ionic strength [28, 29], temperature and solvent effect [30]. A serious question has recently been raised upon the problem of justifying the generalization of relationships between the obtained particles and particular parent microemulsion systems. It was found out [31] that the preparation condition significantly affect both structural properties and crystallization of individual metal oxide mixtures. It is proved [32] that the surface structure of small metal nanocrystals may vary drastically and, as a consequence, their size distribution may play a critical role.

This paper reports on the synthesis of $\text{CeO}_2/\gamma\text{-Al}_2\text{O}_3$

nanopigments via sol-gel process controlled within reverse micelles of non-ionic surfactant Triton X-114 in cyclohexane for the first time. This research focuses on the study of the effect of different calcination temperatures and different molar ratios of Ce:Al on the crystallization, crystallite growth and the phase composition. A quantitative X-ray diffraction phase analysis including estimation of amorphous phase content was also performed.

2. Experimental

Cerium (III) nitrate hexahydrate ($\text{Ce}(\text{NO}_3)_3 \cdot 6\text{H}_2\text{O}$), nanogamma alumina oxide ($\gamma\text{-Al}_2\text{O}_3$), cyclohexane (HPLC grade), nonionic surfactant Triton X-114 ((1, 1, 3, 3,-tetramethyl-buthyl) phenyl-poly ethylene glycol ($\text{C}_{29}\text{H}_{52}\text{O}_{8.5}$)) and absolute ethanol (water content max. 0.2 vol%) were of analytical grade purchased from Sigma Aldrich. Double distilled water was used as precursors in all processes.

Ceria and alumina mixed oxides pigments were prepared via sol-gel processing controlled within reverse micelles of nonionic surfactant Triton X-114 in cyclohexane. Figure 1 shows the preparation flow chart for of $\text{CeO}_2/\gamma\text{-Al}_2\text{O}_3$. Cyclohexane was used as organic solvent. Ceria and alumina mixed oxides pigments with various $\text{CeO}_2:\gamma\text{-Al}_2\text{O}_3$ molar ratios (0.2:3, 0.5:3 and 1:3) were prepared. In the first step, the ceria sol was prepared: 0.13, 0.32 and 0.65 g (for 0.2, 0.5 and 1 mole, respectively) cerium (III) nitrate hexahydrate was dissolved in absolute ethanol (4.5 ml) under intense stirring. In the second step, cyclohexane (24.6 ml) was mixed with Triton X-114 (21.6 ml) and distilled water (0.6 ml) followed by the addition of ceria sol. The sol was stirred for 30 min. In the final step, nanogamma aluminum oxide 0.46 g was fluently injected into the mixture. The micelle ceria/ γ - alumina sol precursor with different molar ratios of Ce:Al was mechanically stirred ($6500 \text{ r} \cdot \text{min}^{-1}$) for 24h at room temperature to form a homogeneous suspension. Then, the homogeneous transparent sol was poured into Petri's dishes in a thin film layer and left in air to be converted into the gel. After that, the mixture was washed with acetone to remove the organic material and dried at 333K for 6h. The powder (metal and supporting agent) was stored in a moisture-free atmosphere. The ceria-alumina sol precursors were prepared keeping the molar ratio of cyclohexane: Triton X-114: H_2O : $\gamma\text{-Al}_2\text{O}_3$: $\text{Ce}(\text{NO}_3)_3 \cdot 6\text{H}_2\text{O}$ at molar ratios and the amount of absolute ethanol was 4.5-7.5

ml, depending on the amount of dissolved molar ratio of Ce:Al. The gelation period of individual ceria-alumina sols differed from 48h to 2 weeks and it showed a strong dependence on ambient temperature and humidity. The gels were thermally treated in air at 623K for 5h and calcined at 823 to 1123K for 5h.

2.1. Characterization

Pigments surface area was determined by N₂

adsorption/desorption isotherm at 77K, using the BET (Brunauer, Emmette and Teller) analysis in a Tristar Micromeritics 3000 flow apparatus. BET surface area was obtained at relative pressure between 0.005 and 0.09. The total pore volume was calculated based on the adsorbed nitrogen volume at the highest relative pressure, while the average pore size diameter was determined by the Barrett, Joyner and Halenda at 523K overnight.

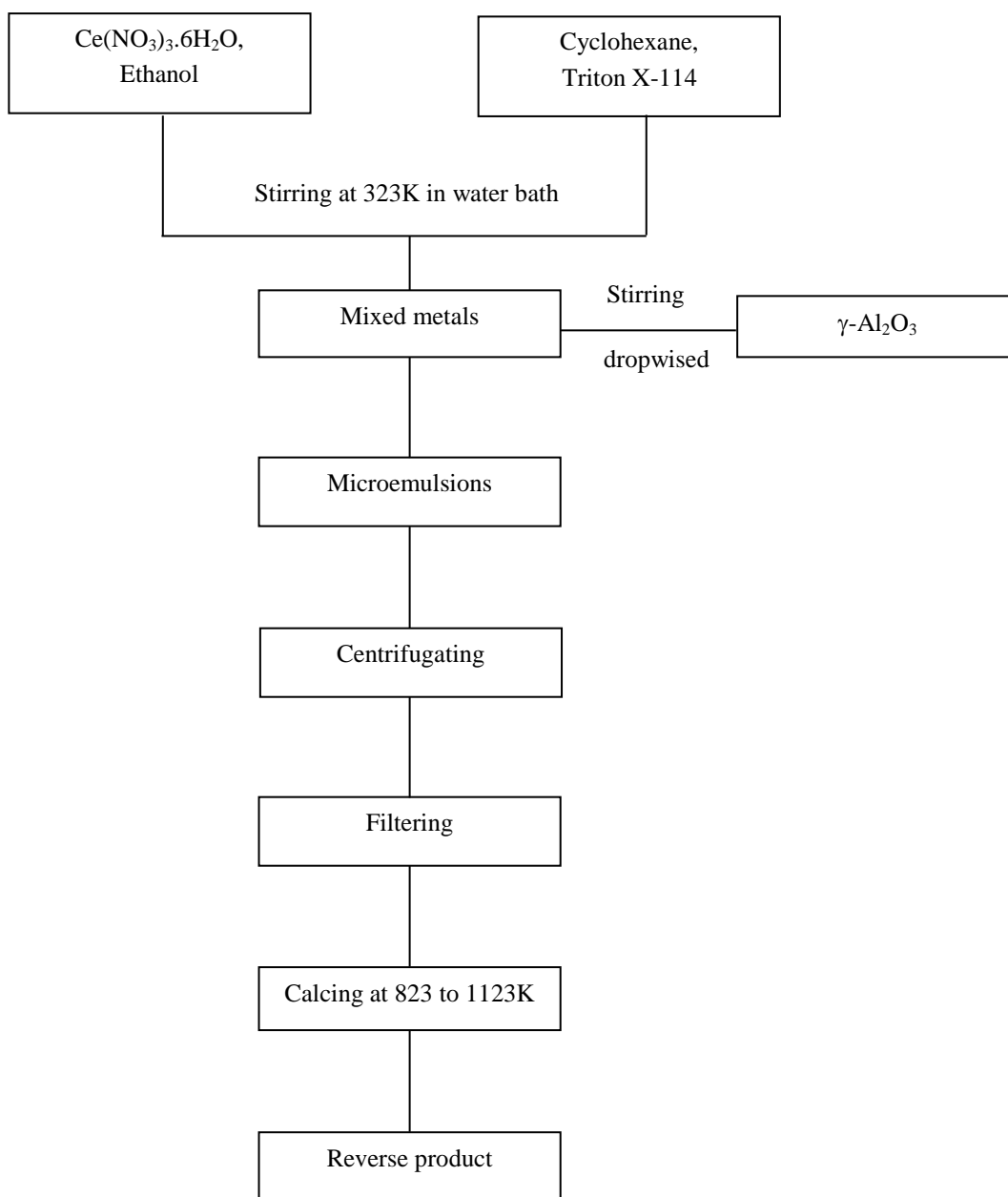


Figure 1: Schematic diagram of synthesize of CeO₂/γ-Al₂O₃ nanoparticles by reverse microemulsion method.

X-ray powder diffraction analysis of the samples was performed on Philips 3100 diffractometer (Koninklijke Philips Electronics N.V., Eindhoven, the Netherlands) using Cu K_{α} radiation. The powders were spread evenly on a 2 mm thick quartz plate. Crystallite size of samples was calculated from full width at half maximum (FWHM) using Scherer's equation. Debye Scherer relation is given as:

$$d = \frac{0.9 \lambda}{\beta \cos \theta} \quad (1)$$

where d is the average crystallite size, β is the full width at half maximum, λ is the X-ray wavelength (1.542 Å) and θ is the angle of diffraction (in radian).

Imaging of the powders was completed using a Hitachi S-4700 scanning electron microscope (Hitachi Ltd., Tokyo, Japan). The powder samples were imaged by dispersing them on carbon tape followed by sputter coating with platinum. Transmission electron microscope (TEM, JEM-2000FX, JEOL) observation was made at an accelerating voltage of 200 kV by placing the powder on a copper grid to get the details about the morphology and size of the powders. The average size of the particles was estimated from the TEM micrograph using standard image analysis software (IMAGE J).

Temperature programmed Reduction (TPR) studies were carried out in a Micrometrics TPR/TPD 2900 instrument equipped with a W-Au thermal conductivity detector and connected to an Olivetti mod. 330-28 acquisition data station at a heating rate of 10 °C min⁻¹.

The reducing agent was a H₂/Ar mixture (5 vol%). The amount of hydrogen consumed was determined upon integration of the areas under the peaks, after calibration of the instrument with CuO (from Merck).

3. Results and Discussions

Figure 2 shows the XRD patterns of the ceria/ γ -alumina precursor with different calcination temperatures (823-1123K) in air for 5h and different molar ratio (0.2:3, 0.5:3 and 1:3). After heating the precursor at 823K in air for 5h, the powder is almost amorphous. Increasing the calcinations temperature to 1123K, the crystallinity increases and CeO₂ and γ -Al₂O₃ phases has been identified. The diffraction peaks become sharper with increasing the temperature indicating the growth of particles. Also, Figure 3 shows the XRD patterns of ceria/ γ -alumina with different molar ratios of Ce:Al calcined at 1123K for 5h. Each crystalline phase was identified using JCPDS. With increasing Ce:Al molar ratio in samples, major diffraction peaks of CeO₂ shifted to lower 2θ value. In addition, XRD peak intensity and crystalline phase of nano-catalysts were affected by the variation of Ce:Al molar ratio. In 0.2:3.0 Ce:Al molar ratio, a small shift of diffraction peaks of cubic CeO₂ to lower 2θ was only observed without phase changing. In (0.5:1.0 and 1.0:3.0 Ce:Al) molar ratios, on the other hand, XRD peaks resulting from the formation of solid solution with cubic phase were gradually developed with increasing Ce:Al molar ratio.

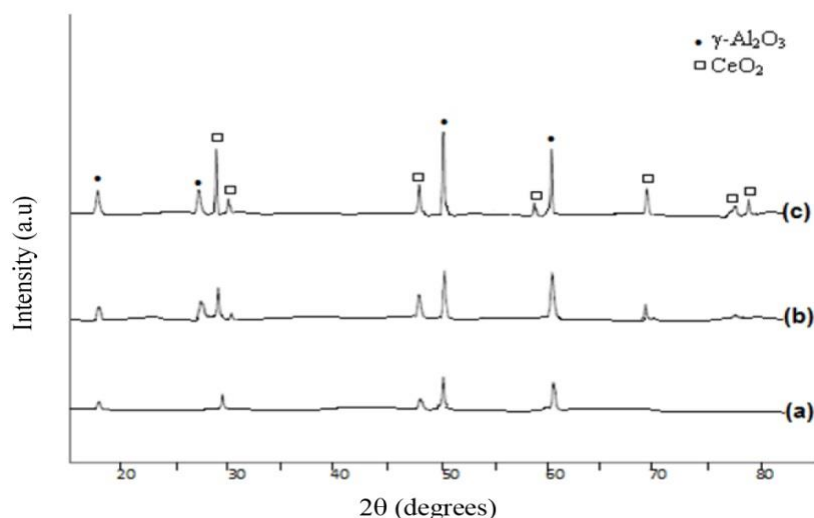


Figure 2: The XRD patterns of CeO₂/ γ -Al₂O₃ at different calcination temperatures; (a) 823, (b) 973 and (c) 1123 K.

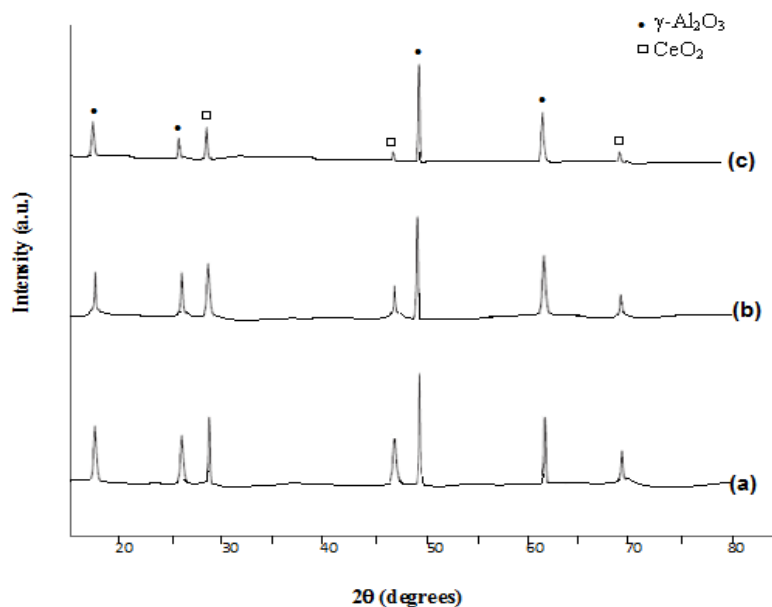


Figure 3: The XRD patterns of CeO₂/γ-Al₂O₃ with different Ce:Al molar ratios at 1123K: (a) 1:3, (b) 0.5:3 and (c) 0.2:3.

Figure 4 shows the TEM images of nanoparticles synthesized with different Ce:Al molar ratios. The inset shows the particle size distribution. The population of particles diameter was determined with using Image J program. 34 particles were measured from TEM micrograph to establish particle size distribution histograms. The histograms were created using Image J with binning widths of 5 nm. The mean sizes and standard deviations resulted from Image J are 20.6 and 4.7 nm, respectively.

Surface area, average particle size and pore volume evaluated by BET, XRD and N₂ adsorption/desorption measurements are shown in Table 1. The average particle size obtained from TEM is bigger than that of Scherer equation. This may be due to the agglomeration of fine particles [33], which occurs not during the chemical synthesizing procedure, but during the isolation of the particles from their parent microemulsion. Table 2 shows molar ratios and phase composition of samples that was determined by SEM-EDX and XRD measurements.

3. Results and discussion

SEM micrographs are shown in Figure 5. By increasing the Ce:Al molar ratio, the particle size decreases

gradually. Also, TEM images provide the same result from SEM images.

TPR measurements were carried out to investigate the reducibility of samples and to see the interaction between metal oxides. Figure 6 shows the TPR profiles of CeO₂/γ-Al₂O₃ pigments with different Ce:Al molar ratios. In the Ce:Al molar ratios of 0.2:3, 0.5:3 and 1:3 as shown in Figure 6 a, b and c, however, broad reduction peaks start from at 633K which is appeared within the range of 903-1453K. Furthermore, continuous H₂ consumption was observed even after the appearance of main reduction peaks. It was reported that CeO₂ phase shows a double reduction peaks at 923 to 1723K. It is found that continuous H₂ consumption at high temperature might cause the sample sintering during the reduction process [34]. It is considered that the shift of reduction peaks to lower temperatures with decreasing the Ce:Al molar ratio can be explained by the fact that highly concentrated Ce⁴⁺ with redox feature enhances the oxygen mobility and oxygen storage capacity [35]. The low-temperature tailing observed in the samples with Ce:Al 0.2:3, 0.5:3 and 1:3 molar ratio might be related to the reduction of CeO_x species weakly interacted with aluminum oxide.

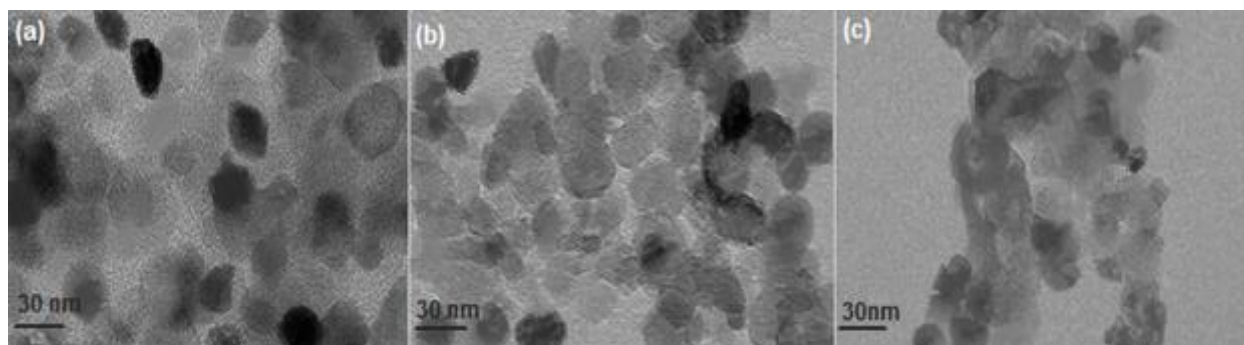


Figure 4. TEM images of $\text{CeO}_2/\gamma\text{-Al}_2\text{O}_3$ with different Ce:Al molar ratios at 1123K; (a) 0.2:3, (b) 0.5:3 and (c) 1:3.

Table 1: Chemical and physical properties of $\text{CeO}_2/\gamma\text{-Al}_2\text{O}_3$ with different molar ratios determined by XRD, BET and N_2 adsorption-desorption measurements.

Supports $\text{CeO}_2/\gamma\text{-Al}_2\text{O}_3$	Average diameter (XRD) (nm)	Particle size (TEM) (nm)	BET surface area (m^2g^{-1})	Pore volume (cm^3g^{-1})
0.2:3.0	21	35	76	0.396
0.5:3.0	32	47	66	0.343
1.0:3.0	44	53	63	0.283

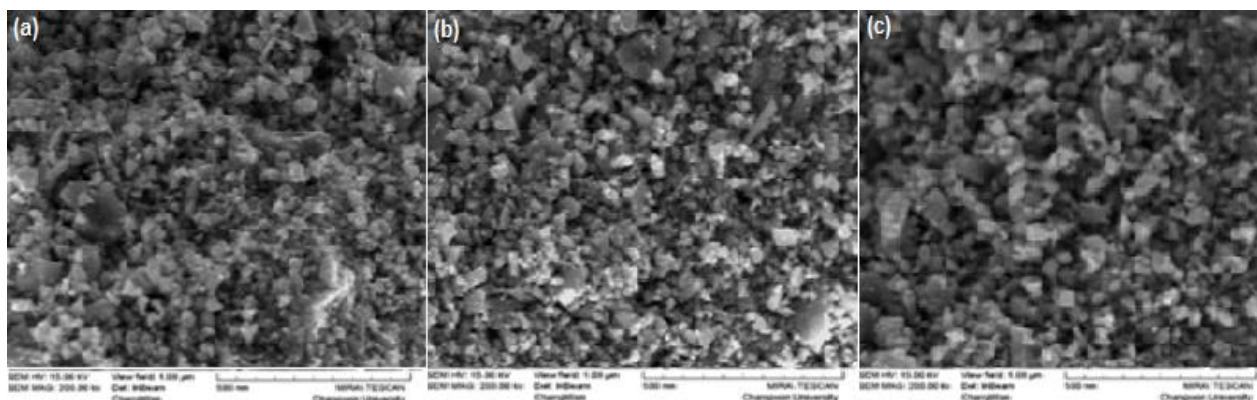


Figure 5: SEM images of $\text{CeO}_2/\gamma\text{-Al}_2\text{O}_3$ with different Ce:Al molar ratios at 1123K; (a) 0.2:3, (b) 0.5:3 and (c) 1:3.

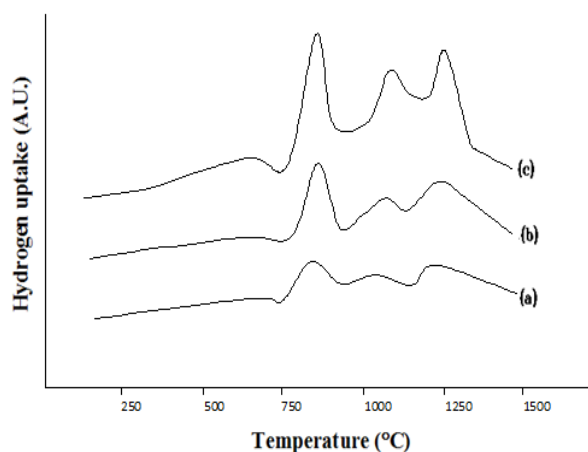


Figure 6: The TPR profiles of $\text{CeO}_2/\gamma\text{-Al}_2\text{O}_3$ with different Ce:Al molar ratios; (a) 0.2:3, (b) 0.5:3 and (c) 1:3.

Table 2: Molar ratio and phase composition of samples determined by SEM-EDX and XRD measurement

Supports CeO ₂ /γ-Al ₂ O ₃	Measured molar ratio CeO ₂ :γ-Al ₂ O ₃ (SEM-EDX)	Phase composition
0.2:3.0	0.24:2.87	γ-Al ₂ O ₃ , CeO ₂
0.5:3.0	0.49:3.11	γ-Al ₂ O ₃ , CeO ₂
1.0:3.0	0.87:3.21	γ-Al ₂ O ₃ , CeO ₂

4. Conclusion

A porous composite of ceria/γ-alumina was successfully synthesized via inverse microemulsion method. Particles size were between 20 to 45 nm at different calcination temperatures and different molar ratios of CeO₂:γ-Al₂O₃. With increasing the calcinations

temperature to 1123K, the crystallinity increases and CeO₂ and γ-Al₂O₃ phases has been identified. The BET surface area decreased by increasing the calcinations temperature. Also, the particle size of the composite samples decreased with increasing the Ce:Al molar ratio

6. References

- J. A. Rodriguez, M. Fernandez-Garcia, Synthesis, Properties and applications of Oxide Nanoparticles, Wiley, New Jersey, 2007, 118-136.
- M. Fernandez-Garcia, A. Martinez-Arias, J. C. Hanson, J. A. Rodriguez, Nanostructured oxides in chemistry: characterization and properties, *Chem. Rev.*, 104(2004), 4063-4104.
- J. A. Rodriguez, G. Liu, T. Jirsak, Z. Hrbek, J. Dvorak, A. Maiti, Activation of gold on titania: adsorption and reaction of SO₂ on Au/TiO₂(110), *J. Am. Chem. Soc.*, 124(2002), 5247-5250.
- V. M. Samsonov, A. N. Bazulev, N. Yu. Sdobnyakov, On applicability of Gibbs thermodynamics to nanoparticles, *Cent. Eur. J. Phys.*, 3(2003), 474-484.
- Z. Song, T. Cai, Z. Chang, G. Liu, J.A. Rodriguez, J. Hrbek, Molecular level study of the formation and the spread of MoO₃ on Au(111) by scanning tunneling microscopy and X-ray photoelectron spectroscopy, *J. Am. Chem. Soc.*, 125(2003), 8059-8066.
- M. D. Hernandez-Alonso, A. B. Hungria, J. M. Coronado, A. Martinez-Arias, J. C. Conesa, J. Soria, M. Fernandez-Garcia, Confinement effects in quasi-stoichiometric CeO₂ nanoparticles, *Phys. Chem. Chem. Phys.*, 6(2004), 3524-3529.
- G. C. Matter, A. Martinez-Arias, Transport Properties and Oxygen Handling in "Synthesis, Properties and Application of Oxide Nanoparticles", Wiley, New Jersey, 2007, 150-164.
- N. Yao, G. Xiong, Y. Zhang, M. He, W. Yang, Preparation of novel mesoporous alumina catalysts by the sol-gel method, *Catal. Today*, 68(2001), 97-109.
- M. Akia, S. M. Alavi, M. Rezaei, Z. F. Yan, Synthesis of high surface area as an efficient catalyst support for dehydrogenation of n-docecane, *J. Porous Mater.*, 17(2010), 85-90.
- K. M. Parida, A. C. Pradhan, J. Das, N. Sahu, Synthesis and characterization of nano-sized porous gamma-alumina by control precipitation method, *Mater. Chem. Phys.*, 113(2009), 244-248.
- T. Noguchi, K. Matsui, N.M. Islam, Y. Hakuta, H. Hayashi, Rapid synthesis of γ-Al₂O₃ nanoparticles in supercritical water by continuous hydrothermal flow reaction system, *Supercritical Fluids*, 46(2008), 129-136.
- A. I. Y. Tok, F. Y. C. Boey, X. L. Zhao, Novel synthesis of Al₂O₃ nano-particles by flame spray pyrolysis, *Mater. Proc. Technol.*, 178(2006), 270-273.
- A. S. Prakash, C. Shivakumara, M. S. Hegde, Single step preparation of CeO₂/CeAlO₃/g-Al₂O₃ by solution combustion method: Phase evolution, thermal stability and surface modification, *Mater. Sci. Ener. B*, 139(2007), 55-61.
- M. Edrissi, R. Norouzbeigi, Preparation of alumina powder via combustion synthesis: porous structure optimization via Taguchi L16 design, *J. Am. Ceram.*, 94(2011), 4052-4058.
- L. Matejova, V. Vales, R. Fajgar, Z. Matej, V. Holy, O. Solcova, Reverse micelles directed synthesis of TiO₂-CeO₂ mixed oxides and

- investigation of their crystal structure and morphology, *J. Solid State Chem.*, 198(2013), 485-495.
16. G. granata, F. Pagnanelli, D. Nishio-Hamane, Nanoparticles of manganese carbonate by microemulsion mediated route: production and characterization, *Appl Surf Sci.*, 331(2015), 463-471.
 17. T. R. Penki, D. Shanmugasundaran, N. Muichandraiah, Porous lithium rich $\text{Li}_{1.2}\text{Mn}_{0.54}\text{Ni}_{0.22}\text{Fe}_{0.04}\text{O}_2$ prepared by microemulsion route as a high capacity and high rate capability positive electrode material, *Electrochimica Acta*, 143(2014), 152-160.
 18. K. Pemartin, C. Solans, J. Alvarez-Auintana, M. Sanchez-Dominguez, Synthesis of Mn-Zn ferrite nanoparticles by the oil-in-water microemulsion reaction method, *Colloids surf A: Physicochem. Eng. Aspects*, 451(2014), 161-171.
 19. M. Hashim, S. E. Shirsath, S. S. Meena, M. L. Mane, S. Kumar, P. Bhatt, R. Kumar, N. K. Prasad, S. K. Alla, J. Shah, R. K. Kotnala, K. A. Mohammed, E. Senturk, Manganese ferrite prepared using reverse micelle process: Structural and magnetic properties characterization, *J. Alloys Compd.*, 642(2015), 70-77.
 20. K. Scherzmanz, Catalysis by Ceria and Related Materials, World Scientific, London, 2002, 212-250.
 21. G. Liu, J.A. Rodriguez, Z. Chang, J. Hrbek, C.H.F. Peden, Adsorption and Reaction of SO_2 on Model $\text{Ce}_{1-x}\text{Zr}_x\text{O}_2(111)$ Catalysts, *J. Phys. Chem. B*, 108(2004), 2931-2940.
 22. A. Trovarelli, Catalytic Properties of Ceria and CeO_2 -Containing Materials, *Catal. Rev. Sci.-Eng.*, 38(1996), 439-520.
 23. J. A. Rodriguez, X. Wang, J. C. Hanson, G. Liu, A. Iglesias-Juez, M. Fernandez-Garcia, The behavior of mixed-metal oxides: structural and electronic properties of $\text{Ce}_{1-x}\text{Ca}_x\text{O}_2$ and $\text{Ce}_{1-x}\text{Ca}_x\text{O}_{2-x}$, *J. Chem. Phys.*, 119(2003), 5659-5666.
 24. Z. Zhang, S. Seal, S. Patil, C. Zha, Q. Xue, Anomalous quasi-hydrostaticity and enhanced structural stability of 3 nm nanoceria, *J. Phys. Chem.*, 111(2007), 11756-11759.
 25. C. C. Wang, D. H. Chen, T. C. Huang, Synthesis of palladium nanoparticles in water-in-oil microemulsions, *Colloid Surf A*, 189(2001), 145-150.
 26. E. E. Carpenter, C. T. Seip, C. J. O'Connor, Magnetism of nanophase metal and metal alloy particles formed in ordered phases, *J. Appl. Phys.*, 85(1999), 5184-5186.
 27. J. Chandradass, M. Balasubramanian, D. S. Bae, J. Kim, K. H. Kim, Effect of water to surfactant ratio (R) on the particle size of MgAl_2O_4 nanoparticle prepared via reverse micelle process, *J. Alloys Compd.*, 491(2010), L25-L28.
 28. X. H. Yang, Q. S. Wu, L. Li, Y. P. Ding, G. X. Zhang, Controlled synthesis of the semiconductor CdS quasi nanospheres, nanoshuttles, nanowires and nanotubes by the reverse micelle systems with different surfactants, *colloids surf A: Physicochem. Eng. Aspects*, 264(2005), 172-178.
 29. R. Jusoh, A. A. Jalil, S. Triwahyono, A. Idris, S. Haron, N. Sapawe, Synthesis of reverse micelle $\alpha\text{-FeOOH}$ nanoparticles in ionic liquid as an only electrolyte: inhibition of electron-hole pair recombination for efficient photoactivity, *Appl. Catal. A: General*, 469(2014), 33-44.
 30. J. Chandradass, K. Hyeon Kim, Solvent effects in the synthesis of MgFe_2O_4 nanopowders by reverse micelle processing, *J. Alloys compd.*, 509(2011), L59-L62.
 31. P. H. Holgado, M. J. Holgado, M. S. San Roman, V. Rives, Effect of surfactants on the properties of hydrotalcites prepared by the reverse micelle method, *Mater. Chem. and Phys.*, 151(2015), 140-148.
 32. R. A. Van Santen, Complementary structure sensitive and insensitive catalytic relationships, *ACC. Chem. Res.*, 42(2009), 57-66.
 33. J. Chandradass, K. Ki Hyeon, Mixture of fuels approach for the solution combustion synthesis of LaAlO_3 nanopowders, *Adv. Powder Technol.*, 21(2010), 100-105.
 34. M. Daturi, E. Finocchio, C. Binet, J. C. Lavalley, F. Fally, V. Perrichon, Reduction of high surface area $\text{CeO}_2\text{-ZrO}_2$ mixed oxides, *J. Phys. Chem. B*, 104(2000), 9186-9194.
 35. K. W. Jun, H. S. Roh, K. V. R. Chary, Structure and catalytic properties of ceria-based nickel catalysts for CO_2 reforming of methane, *Catal. Surv. Asia.*, 11(2007), 97-113.

How to cite this article:

R. Lotfi, S. Abedini Khorrani, M. E. Olya, Sh. Moradi, F. Motiee, Effect of molar ratio and calcination temperature on particle size of $\text{CeO}_2/\gamma\text{-Al}_2\text{O}_3$ nanocomposites prepared via reverse micelle process, *Prog. Color Colorants Coat.*, 9 (2016) 109-116.

